Multiple-photon effects in fermion-(anti)fermion scattering at Superconducting Super Collider energies

D. B. DeLaney, S. Jadach,* Ch. Shio, G. Siopsis, and B. F. L. Ward

Department of Physics and Astronomy, The University of Tennessee, Knoxville, Tennessee 37996-1200

We use the theory of Yennie, Frautschi, and Suura to realize, via Monte Carlo methods, the process $f\,{}^{(\overline{-})}_{f} \to f'\,{}^{(\overline{-})'}_{f} + n\gamma$ at energies reached at the Superconducting Super Collider (SSC) and the CERN Large Hadron Collider, where f and f' are quarks or leptons. QED infrared divergences are canceled to all orders in perturbation theory. The resulting Monte Carlo event generator SSC-YFS2 is used to study the effects of initial-state photon radiation on these processes in the SSC environment. Sample Monte Carlo data are presented and discussed. We find that the respective multiple-photon effects must be taken into account in discussing precise predictions for SSC physics processes.

PACS number(s): 13.40.Ks, 13.10.+q, 13.85.−t

I. INTRODUCTION

Now that the Superconducting Super Collider (SSC) is under construction, it is extremely important to prepare for the maximal physics utilization and exploration of the new frontier which it will probe. In particular, it is of some import to determine the effects of higher-order radiative corrections on the SSC physics processes of interest so that optimal discrimination between signal and background can be realized. In this paper, we explore the first step in the determination of such corrections by computing them for the basic QED-related effects in $f\bar{f} \to f'\bar{f}' + n\gamma$ at SSC energies using the methods which two of us (S.J. and B.F.L.W.) introduced for the analogous processes $e^+e^- \to f\bar{f} + n\gamma$ for high precision Z^0 physics at the SLAC Linear Collider (SLC) and CERN e^+e^- collider LEP. Thus, here, we extend the SLC and/or LEP Monte Carlo event generator YFS2 in the first paper in Ref. [1] to the SSC physics environment. An analogous study of the multiple-gluon radiation in SSC processes such as $qq \to q'q' + nG$ (where q, q' represent quarks and G a gluon) will appear elsewhere [2].

In the SSC environment, multiple-photon and multiple-gluon radiative effects are expected to be important, in partial analogy with the significance of multiple-photon radiation in the SLC and LEP environments. The analogy is partial because the would-be resonance at the SSC, the Higgs boson, is actually quite broad compared to the Z^0 at SLC and LEP. Nonetheless, if $\bar{k}_0 \approx 0.001\sqrt{s}/2$ is a typical infrared resolution factor for an SSC detector, then the probability of an incoming u quark to radiate at the SSC is, e.g.,

$$P(\bar{k}_0 \le k \le \sqrt{s}/2) \approx \frac{2\alpha Q_u^2}{\pi}[\ln(\sqrt{s}/6m_u)^2 - 1]\ln(\sqrt{s}/\bar{k}_0)$$
$$= 0.44 , \tag{1}$$

where $\sqrt{s} = 40$ TeV and $m_u \sim 5.1$ MeV. Hence, such radiation and its attendant effect on the respective SSC event structure must be computed to the standard SLC/LEP precision to assess its interplay with detector cuts, physics signals and physics backgrounds. This would then leave only the multiple-gluon radiative effects to be taken into account to gain a complete view of higher-order radiative effects to SSC physics processes. Such gluon radiation will be taken up elsewhere [2].

Our strategy is to treat the incoming quark radiation via the Yennie-Frautschi-Suura (YFS) theory [3] so that we realize it on an event-by-event basis using the methods in Ref. [1]. The full multiple-photon character of the final state, including the physical four-momentum vectors of the photons, is then made available to the users of the attendant new multiple-photon event generator SSC-YFS2. The implementation of arbitrary detector cuts on the respective simulated cross sections is straightforward.

A logical next step is to include the effects of the final-state multiple-photon radiation via the extension of the Monte Carlo event generators BHLUMI2.0 [1, 4] and YFS3 [5] to the SSC environment in analogy with our extension of YFS2 in the current work. We shall discuss these extensions in a future publication [2].

Our work is organized as follows in the paper: in the next section, we review the YFS methods as they are implemented in YFS2 in the first paper in Ref. [1], so that this paper is self-contained; in Sec. III, we discuss how we extend YFS2 to SSC processes and energies to get the Monte Carlo event generator SSC-YFS2; in Sec. IV, we present some sample Monte Carlo data for SSC physics processes and comment on their implications; finally, in Sec. V, we present our outlook and summary remarks.

II. REVIEW OF YFS METHODS

In this section, we review the methods used in Ref. [1] to realize the YFS theory via the Monte Carlo event generator YFS2 for $e^+e^- \to f\bar{f} + n\gamma$, $f \ne e$, in the Z^0 energy regime. We begin by recalling the key ingredients of these methods.

*Permanent address: Institute of Physics, Jagellonian University, Cracow, Poland.

The YFS Monte Carlo methods in Ref. [1] take advantage of the expansion of the total cross section for the process illustrated in Fig. 1,

$$e^+(p_1) + e^-(p_2) \longrightarrow f(q_1) + \bar{f}(q_2)$$
$$+\gamma(k_1) + \cdots + \gamma(k_n) \ , \qquad (2)$$

in terms of the YFS hard-photon residuals [3] $\bar{\beta}_n(k_1, \ldots, k_n)$, which are free of all virtual and real infrared divergences to all orders in the QED coupling constant α, and of the products of the YFS infrared emission factors [3]

$$\widetilde{S}(k) = -\frac{\alpha}{4\pi^2}\left(\frac{p_1}{p_1 \cdot k} - \frac{p_2}{p_2 \cdot k}\right)^2 + \cdots \ , \qquad (3)$$

where the ellipsis represents the remaining terms obtained from that shown by the appropriate substitutions of $\{(e, p_1), (-e, p_2)\}$ with $\{(Q_f e, q_1), (-Q_f e, q_2)\}$, with
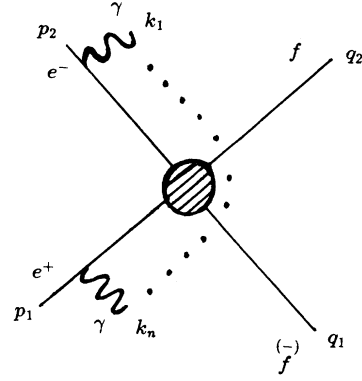

FIG. 1. The process $e^+(p_1) + e^-(p_2) \to f(q_2) + \bar{f}(q_1) + \gamma(k_1) + \cdots + \gamma(k_n)$.

due attention to signs associated with the direction of the flow of charge. The most infrared-singular contribution to the cross section involves n factors of $\widetilde{S}$, as we see from the following expression for the respective cross section:

$$d\sigma^{(n)} = \left(\widetilde{S}(k_1) \cdots \widetilde{S}(k_n)\bar{\beta}_0(p_1, p_2, q_1, q_2) + \cdots + \bar{\beta}_n(k_1, \ldots, k_n)\right)$$
$$\times \frac{1}{n!}\delta^4\left(p_1 + p_2 - q_1 - q_2 - \sum_{i=1}^{n} k_i\right)\frac{d^3q_1}{q_1^0}\frac{d^3q_2}{q_2^0}\frac{d^3k_1}{k_1^0}\cdots\frac{d^3k_n}{k_n^0}\,e^{2\alpha\,\mathrm{Re}B} \ , \qquad (4)$$

where B is the YFS virtual infrared function and is given in Refs. [1] and [3]. Basing ourselves on (4), in YFS2 we proceed as follows.

We use the YFS form factor

$$F_{\mathrm{YFS}}(p_1, p_2, \epsilon) = \exp\left(2\alpha\,\mathrm{Re}B + \int\frac{d^3k}{k^0}\widetilde{S}(p_1, p_2, k)\left[1 - \theta(k^0 - \epsilon\sqrt{s}/2)\right]\right)$$
$$= \exp\left(\frac{\alpha}{\pi}[2(\ln(s/m_e^2) - 1)\ln\epsilon + \tfrac{1}{2}\ln(s/m_e^2) - 1 + \pi^2/3]\right) \ , \qquad (5)$$

to compensate for the omission of small-energy photons with $k^0 < \epsilon\sqrt{s}/2$ for $\epsilon \ll 1$ from the phase space in (4) to all orders in α, as is effected by inserting $\prod_{i=1}^{n}\theta(2k_i^0/\sqrt{s} - \epsilon)$ into (4) and summing over all $d\sigma^{(n)}$. Here we presume we are in the e^+e^- center-of-mass frame. For YFS2, the hard photon residuals $\bar{\beta}_{0,1,2}$ are used, as two of us have explained in Ref. [1]. This means that, in the YFS2 Monte Carlo program itself, some choice must be made for the reduction of the n-photon+$f\bar{f}$ phase space to the j-photon+$f\bar{f}$ phase space $(n = 0, 1, 2, \ldots, j = 0, 1, 2, n \geq j)$, which is involved in the definition of the residuals $\bar{\beta}_i$ $(i = 0, 1, 2)$. We call this choice the reduction procedure $\mathcal{R}$ and the exact YFS result $\sum_n d\sigma^{(n)}$ is independent of it, if it is done according to the rigorous YFS theory. Our choice for $\mathcal{R}$ is explained in [1]. Finally, we should emphasize that, for efficient event generation, it is always desirable to generate a background population of events according to a set of distributions $d\sigma'^{(n)}$ which embody all of the general features of Eq. (4), but which remove unnecessary details, and to restore the exact distributions $d\sigma^{(n)}$ in (4) by rejection methods. In Refs. [1] we follow this strat-

egy in constructing YFS2; in addition, several changes of variables are used to make the background generation simpler and more efficient from the standpoint of CPU time. In this way we have realized the YFS theory for $e^+e^- \to f\bar{f} + n\gamma$ with $\bar{\beta}_0$, $\bar{\beta}_1$, and $\bar{\beta}_2$, where we should emphasize that $\bar{\beta}_2$ has only been included in the second-order leading-log approximation [6].

In the next section, we discuss how we extend YFS2 to more general incoming $f\bar{f}$ and ff initial and final states, as well as the modifications needed to make the program applicable in the SSC energy regime.

III. YFS2 AT SSC ENERGIES

In this section we describe how one extends the YFS2 Monte Carlo program in Ref. [1] to realize particle interaction at SSC energies. Such an extension involves the introduction of new physics (mainly through a modification of the Born cross section), numerical problems (due to the very high energies involved, care is needed for the accuracy of the formulas), and certain technical problems associated with the Monte Carlo weight rejection method.

We begin by discussing the modifications made to introduce the new physics at SSC energies. The new program SSC-YFS2 computes the cross section for the interaction

$$f(p_1) + \overset{(-)}{f}(p_2) \longrightarrow f'(q_1) + \overset{(-)}{f}{}'(q_2)$$
$$+\gamma(k_1) + \cdots + \gamma(k_n) , \tag{6}$$

where f is any lepton or quark.[1] This is still not the most general form of SSC interactions, because the incoming fermions are of the same type (identical or particle-antiparticle pair). We are currently generalizing the program to include all interactions, and shall report on the results shortly [2].

The mass parameters m_q used for the quarks are the Lagrangian quark masses [7]. We have in mind that the overall momentum transfer in the interactions will be large compared to the typical momenta inside the proton. In fact, these quark mass parameters should strictly speaking be running masses $m_q(\mu)$, where μ is the scale at which they are being probed. Such a running mass effect is well known and is readily incorporated in the program, as the accuracy one is interested in may dictate. Thus, with this understanding, further explicit reference to the running mass effect is suppressed and all of our results will be evaluated with m_q evaluated at scale $\mu = 1$ GeV as they are given by Gaisser and Leutwyler in Ref. [7]. We have checked that the attendant aproximation is within the level of accuracy of our work in this paper.

The interactions realized by YFS2 [Eq. (2)] involve only an exchange of γ and Z^0 in the s channel. For SSC-YFS2, realizing the more general interaction (6), γ, Z^0, and $W^\pm$ exchange in the t and u channels, accordingly, had to be introduced. This was done by generalizing the Born cross section to include the additional channels. Moreover, in the case of quark interactions, a gluon exchange was added in all three channels. The running strong coupling constant (evaluated at the momentum transfer of the respective hard scattering process)

$$\alpha_s(\mu) = \frac{12\pi}{(33 - 2n_f) \ln\{\mu^2/(\Lambda_{n_f}^{\overline{MS}})^2\}} , \tag{7}$$

was used, where n_f is the number of quark flavors below the energy level μ and $\overline{MS}$ denotes the modified minimal subtraction scheme. In our case, $n_f = 6$, and therefore the QCD parameter $\Lambda_6^{\overline{MS}}$ is used. It can easily be related to the experimentally measured parameter $\Lambda_4^{\overline{MS}} = 238$ MeV:

$$\Lambda_6^{\overline{MS}} = \Lambda_5^{\overline{MS}} \left(\frac{\Lambda_5^{\overline{MS}}}{m_t} \right)^{2/21} , \quad \Lambda_5^{\overline{MS}} = \Lambda_4^{\overline{MS}} \left(\frac{\Lambda_4^{\overline{MS}}}{m_b} \right)^{2/23} .$$
$$\tag{8}$$

The masses of the top and bottom quarks were set to $m_b = 5$ GeV and $m_t = 250$ GeV, respectively, but the results are little affected by their precise values. It is also true that our $n(\gamma)$ effects are relatively insensitive to the value of n_f; the user can specify this as needed.

Certain numerical problems arise at very high energies, because of the very small value of all ratios $m/\sqrt{s}$, where m is the mass of any interacting particle, and $\sqrt{s} = 40$ TeV is the energy of the incoming fermions in their center-of-mass frame. Certain formulas had to be rewritten so that such small numbers would not be ignored by the computer when they should not be; if one is not careful, ratios of the form 0/0 appear at various places. Working at SSC energies, however, has the advantage that all terms of order m^2/s or higher can be dropped. The error is negligible and leads to a considerable simplification of formulas, and consequently to a reduction in computer time.

Next we discuss the event-generation procedure. To perform the integration for the total cross section, we first simplify the form of the differential cross section. Thus the exact cross section $d\sigma$ is replaced by $d\sigma'$, so that the integral $\int d\sigma'$ can be performed analytically. The exact cross section is then computed by rejecting events according to their weights:

$$w = \frac{d\sigma}{d\sigma'} . \tag{9}$$

Apart from simplicity, we require that $d\sigma'$ lead to an efficient generation of events. In YFS2, $d\sigma'$ was chosen to be a constant. In the present case, this is no longer possible, because of the presence of the t channel. The cross section has a singularity at $t \equiv (p_1 - q_1)^2 = 0$ of the form $1/t^2$. To account for the singularity, an angle cutoff $\theta_0 = 100$ mrad is introduced. This is in accord with current detector capabilities, and can be changed at will. A crude cross section $d\sigma'$ of the form

$$d\sigma' = A + \frac{B}{t^2} , \tag{10}$$

was chosen, where the constants A and B depend on the interaction.[2] When a u channel also contributes, a similar term of the form $1/u^2$ must be added to account for the singularity at $u \equiv (p_1 - q_2)^2 = 0$.

Finally, we comment on the choice of the reduction procedure which is needed for the definition of the arguments of the YFS residuals $\bar{\beta}_i$ ($i = 0, 1, 2$), as explained in Sec. II. The reduction procedure is more delicate in the presence of the t channel, due to the singularity at $t = 0$. One has to make sure that the weights (9) do not become uncontrollably large. This is managed by making t as large as possible after the reduction. It is not always possible to increase the reduced t so that the weight (9) remains below the maximum weight. The object of this exercise is to minimize the error originating from the tail

---

[1]At present, the program cannot handle third-generation fermions.

[2]A fictitious photon mass cutoff was also tested, but it turned out to lead to a large weight rejection rate.

of the distribution of weights above the maximum weight (which is set to 3, but can be changed if so desired). This is accomplished by a somewhat involved reduction procedure, which is an adaptation of the similar procedure in BHLUMI1.xx [8]. [We note that two of us (S.J. and B.F.L.W.) have shown in Ref. [1] that the reduction procedure used in SSC-YFS2 really does not affect the respective Monte Carlo results at the level of accuracy of the program. Indeed, in Refs. [1] and [4], two different reduction procedures are used in BHLUMI1.xx and BHLUMI2.01, with no change in the normalization to 0.15%, which is the expected size of the second-order bremsstrahlung corrections which are not represented by the $\beta_{0,1}$ in BHLUMI. Similarly, we find here that the use of these two versions of the reduction procedure does not affect our results to the level of the missing third-order corrections not represented by $\beta_{0,1,2}$, which is below 0.1%.]

This concludes our discussion of the modifications in the YFS2 program necessary in order to realize interactions at SSC energies. Next, we present some of our results.

IV. MULTIPLE-PHOTON EFFECTS AT SSC ENERGIES

In this section we present some results on the effects of multiple-photon initial-state radiation on the incoming qq and $q\bar{q}$ "beams" at SSC energies using our YFS Monte Carlo event generator SSC-YFS2 Fortran. Our objective is to determine the size of these effects with an eye toward their incorporation into SSC physics event generators. This latter step will be taken up elsewhere [2].

We consider, as illustrated in Fig. 2 (the kinematics is summarized in the figure),

$$q(p_1) + {}^{(}\bar{q}{}^{)}(p_2) \longrightarrow q'(q_1) + {}^{(}\bar{q}{}^{)'}(q_2)$$
$$+\gamma(k_1) + \cdots + \gamma(k_n) , \qquad (11)$$

at $\sqrt{s} = 40$ TeV for $q, q' = u, d, s$. For definiteness, we will illustrate our results with $q = u, d$, where we use $m_u = 5.1 \times 10^{-6}$ TeV, $m_d = 8.9 \times 10^{-6}$ TeV, and view $\sqrt{s} = 40$ TeV as our worst-case scenario. The more typical [9] value $\sqrt{s} \approx \frac{1}{6}40$ TeV ≈ 6.7 TeV is also presented
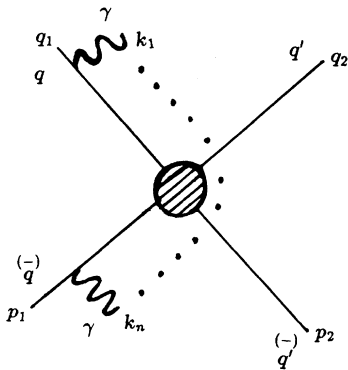
here for completeness. For these respective input scenarios, we shall discuss the following distributions: the number of photons per event, the value of $v = (s - s')/s$, where $s' = (q_1 + q_2)^2$, and the squared transverse momentum of the outgoing $n\gamma$ state. These distributions give us a view of the effect of this multiple-photon radiation on the incoming quarks and (anti)quarks in the SSC environment, where one is really interested in $p\bar{p} \to H + X$, where H is the standard model Higgs particle.

Considering first the number of photons per event, we have the results in Fig. 3. There, we show that for the uu incoming beams, the mean number $\langle n_\gamma \rangle$ of radiated photons is 0.85 ± 0.92 (it is similar for $\sqrt{s} = 6.7$ TeV). This should be compared to the dd incoming state, where $\langle n_\gamma \rangle$ is 0.21 ± 0.45. For reference, we recall [1] that at LEP/SLC energies, the corresponding value of $\langle n_\gamma \rangle$ is,

FIG. 2. The SSC process $q(q_1) + {}^{(}\bar{q}{}^{)}(p_1) \to q'(q_2) + {}^{(}\bar{q}{}^{)'}(p_2) + \gamma(k_1) + \cdots + \gamma(k_n)$, where $q, q' = u, d, s$.
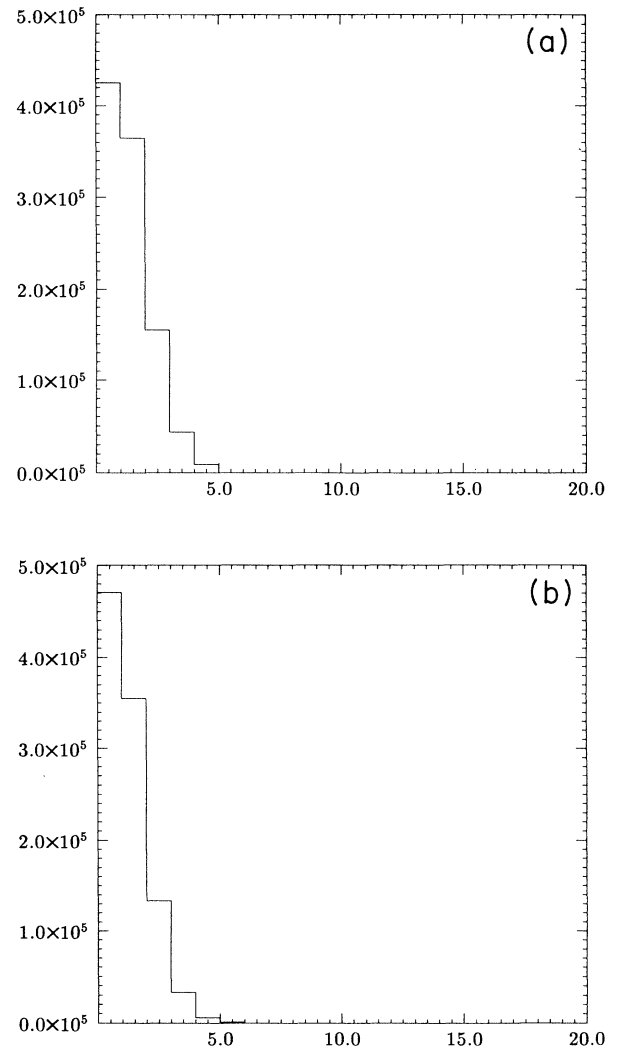

FIG. 3. Histogram of the photon multiplicity in $uu \to uu + n\gamma$ for $|\eta| < 2.8$: (a) $\sqrt{s} = 40$ TeV; (b) $\sqrt{s} = 6.7$ TeV. Here, $v_{min} = 10^{-6}$—we have shown in Ref. [1] that the cross section does not depend on v_{min}.

for the incoming e^+e^- state, $\sim 1.5 \pm 1.0$. Hence, we see here one immediate effect of the high energy of the SSC incoming beams: the initial uu-type state will radiate a significant number of real photons, with a consequent change in the observed final-state character. In particular, the issue of how much energy is lost to photon radiation is of immediate interest, for this energy is unavailable for Higgs-boson production by uu (or dd) and, further, it may fake a signal of $H \rightarrow \gamma\gamma$ if we are unlucky. Accordingly, we now look at the predicted distribution of

$$v \equiv (s - s')/s , \tag{12}$$

where $s' = (q_1+q_2)^2$ is the squared invariant final fermion pair mass. If only one photon is radiated, v is just the energy of this photon in the center-of-mass system of the incoming beams (in units of the incoming beam energy). What we find for v is shown in Fig. 4 for the $uu \rightarrow$

$uu+n\gamma$ case (the $dd \rightarrow dd+n\gamma$ case is similar). We see the expected shape of v from Ref. [1], and its average value is $\langle v \rangle = 0.05 \pm 0.09$. Hence, $\sim 10\%$ of the incoming energy is radiated into photons; this energy is not available for Higgs production and hence it is crucial to fold our radiation into the currently available SSC Higgs production Monte Carlo event generators [10] and to complete the development of our own YFS multiple-photon (-gluon) Higgs production Monte Carlo event generator, which is under development and will appear elsewhere [2].

Given that we know we have, in the SSC environment, significant multiple-photon radiation effects, the question of immediate interest is how often the transverse momenta of two photons are large enough that they could fake a $H \rightarrow \gamma\gamma$ signal. We will answer this very important question in detail in the not-too-distant future when our complete Higgs production YFS Monte Carlo event generators are available [2]. However, here we can begin
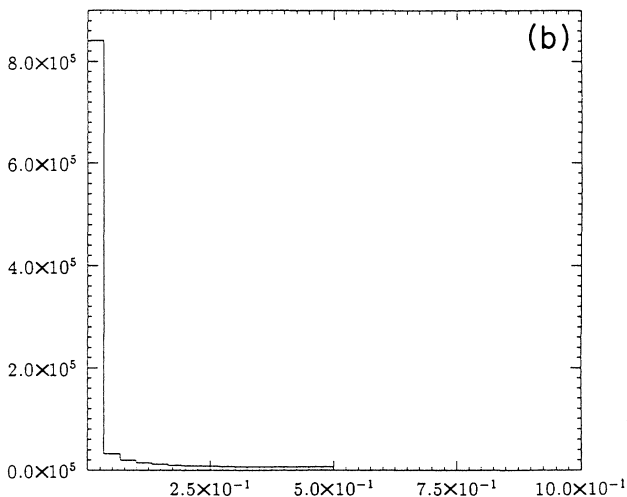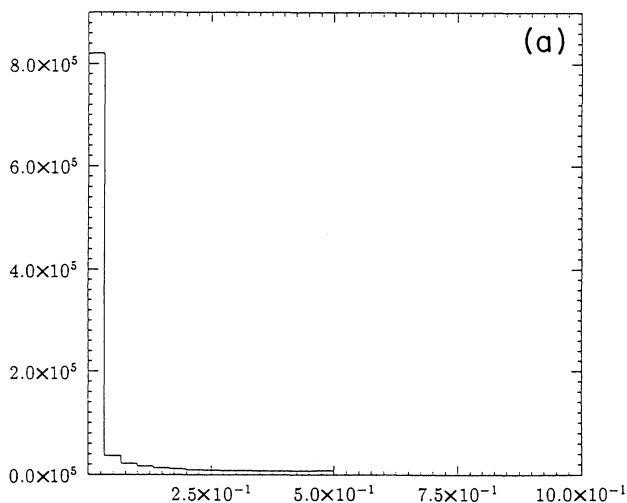

FIG. 4. v distribution for $uu \rightarrow uu + n\gamma$, where $v = (s - s')/s$ and $s' = (q_1 + q_2)^2$ is the squared final uu invariant mass. Here, $|\eta| < 2.8$: (a) $\sqrt{s} = 40$ TeV; (b) $\sqrt{s} = 6.7$ TeV.
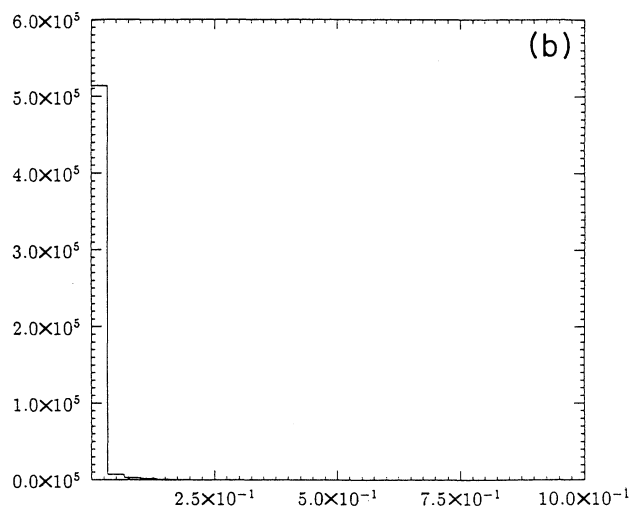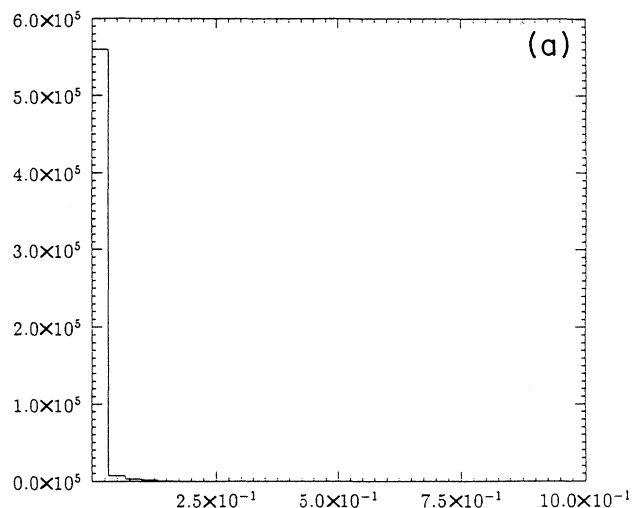
FIG. 5. Total transverse momentum distribution of the photons in $uu \rightarrow uu + n\gamma$ for $|\eta| < 2.8$ in units of s: (a) $\sqrt{s} = 40$ TeV; (b) $\sqrt{s} = 6.7$ TeV.

TABLE I. Sample output for $uu \to uu + n\gamma$ at $\sqrt{s} = 40$ TeV and $|\eta| < 2.8$. The entries in the table are largely explained therein: XSEC = cross section, WT = event weight, and BORN = Born cross section. NEV = of events.

	EXPAND OUTPUT - WINDOW A		
40 000.000 000 000	CMSENE	CMS ENERGY	
	TOTAL XSEC FROM MONTE CARLO		
141 382.572 346 904	XSMC	IN R UNITS	A0
42.706 621 844		ABSOLUTE ERROR	A1
7.674 924 695	XSMCPB	IN PICOBARNS	A2
0.002 318 320		ABSOLUTE ERROR	A3
0.000 302 064	EREL	RELATIVE ERROR	A4
3 308 257	NEVTOT	NO OF EVENTS - TOTAL	A5
1 000 000	NEVACC	ACCEPTED	A6
7	NEVNEG	WITH NEGATIVE WEIGHT	A7
1 903	NEVOVE	WITH WT > WTMAX	A8
6.883 329 409	XBORNB	BORN IN PICOBARNS	A9
126 800.308 378 648	XBORNC	BORN	A9

to study this question by looking into the transverse momentum distribution of our YFS multiple-photon radiation in, e.g., $uu \to uu+n\gamma$. This is shown in Fig. 5, where we plot the total transverse momentum distribution of the respective YFS multiple-photon radiation. What we find is that, for $\sqrt{s} = 40$ TeV, the average value of this total transverse momentum is (in the incoming uu center-of-mass system)

$$\langle k_{\perp,\text{tot}} \rangle \equiv \left\langle \left| \sum_{i=1}^{n} \mathbf{k}_{i\perp} \right| \right\rangle = (0.0184 \pm 0.0129)\sqrt{s} , \quad (13)$$

where k_i $(i = 1,\ldots,n)$ are the four-momenta of the n photons. [For $\sqrt{s} = 6.7$ TeV, this average is $(0.0186 \pm 0.0136)\sqrt{s}$.] Hence, for the Solenoidal Detector Collaboration (SDC) acceptance cut [the Gamma Electron Muon (GEM) Collaboration would have a similar cut] of $\frac{1}{2}|\ln\tan(\theta/2)| \equiv |\eta| < 2.8$, or $\theta_i > 122$ mrad, this means that there may be some possible background to $H \to \gamma\gamma$ for, e.g., $m_H \approx 150$ GeV. Such effects will be discussed in detail elsewhere [2].

Finally, concerning the overall normalization, we find that the Born cross section is corrected according to the results in Table I. This shows clearly that the higher-order effects change the normalization by approximately 5%. This sets the level at which precise simulations of SSC physics must take the higher-order effects from multiple photons into account.

V. CONCLUSIONS

We conclude that our initial study of YFS multiple-photon radiation in the SSC physics environment shows that any Monte Carlo event generator which hopes to achieve an accuracy of order 10% in the SSC physics simulations must treat the respective effects in a complete way. In this paper, we have computed these effects for incoming quark-(anti)quark states at SSC energies using the Monte Carlo event generator SSC-YFS2 based on our original YFS2 Monte Carlo program in Ref. [1].

Specifically, using our SSC-YFS2 Monte Carlo event generator for $q^{(\bar{q})} \to q'^{(\bar{q})'} + n\gamma$, at $\sqrt{s} = 40$ TeV, we find that for an initial uu state, the mean number of radiated photons is 0.85 ± 0.92, so that the multiple-photon character of the events must be taken into account in detailed detector simulation and physics analysis studies. Further, the mean value of $v = (s-s')/s$ is 0.05 ± 0.09 and the average total squared transverse momentum $\langle k_{\perp,\text{tot}} \rangle$ is 0.018 ± 0.013 s. Hence, the impact of these event characteristics on Higgs production in general and on the $H \to \gamma\gamma$ scenario in particular must be assessed in detail. Such assessment will appear elsewhere [2].

In conclusion, we can say that the initial platform for precision SSC electroweak physics simulations on an event-by-event basis using our YFS Monte Carlo approach [1] has now been established. We look forward with excitement to its complete development for all such electroweak phenomena and to its extension to the SSC QCD processes as well [2].

ACKNOWLEDGMENTS

[1] See, e.g., S. Jadach and B. F. L. Ward, Comput. Phys. Commun. **56**, 351 (1990); Phys. Rev. D **40**, 3582 (1989); **38**, 2897 (1988), and references therein.

[2] D. B. DeLaney *et al.* (unpublished).

[3] D. R. Yennie, S. C. Frautschi, and H. Suura, Ann. Phys. (N.Y.) **13**, 379 (1961).

[4] S. Jadach *et al.*, Phys. Lett. B **268**, 253 (1991); Comput. Phys. Commun. **70**, 305 (1992); Phys. Rev. D **44**, 2669 (1991).

[5] S. Jadach and B. F. L. Ward, Phys. Lett. B **274**, 470 (1992); and (unpublished).

[6] S. Jadach *et al.*, Phys. Rev. D **42**, 2977 (1990).

[7] We use the definition of Lagrangian quark masses as given by S. Weinberg, in *Festschrift for I. I. Rabi*, edited by L. Motz (New York Academy of Sciences, New York,

1977), and by J. Gaisser and H. Leutwyler, Phys. Rep. **87**, 77 (1982), so that the values of these masses at the scale $\mu = 1$ GeV are taken from the latter authors.

[8] S. Jadach and B. F. L. Ward, Phys. Rev. D **40**, 3582 (1989).

[9] See, e.g., E. Eichten *et al.*, Rev. Mod. Phys. **56**, 579 (1984).

[10] See, e.g., F. E. Paige and D. Protopopescu, in *Physics of the Superconducting Super Collider, Snowmass, 1986*, Proceedings of the Summer Study, Snowmass, Colorado, 1986, edited by R. Donaldson and J. Marx (Division of Particles and Fields of the APS, New York, 1988), p. 320; H.-U. Bengtsson and T. Sjostrand, Comput. Phys. Commun. **46**, 43 (1987).